Microwave resonant electro-optic bulk phase modulator for two-dimensional smoothing by spectral dispersion in SG-II

Youen Jiang (姜有恩)*, **Xuechun Li (李学春)**, **Shenlei Zhou (周申蕾)**, **Wei Fan (范　薇)**, **and Zunqi Lin (林尊琪)**

National Laboratory of High Power Laser Physics, Shanghai Institute of Optics and Fine Mechanics, Chinese Academy of Sciences, Shanghai 201800, China

**Corresponding author: joyen@siom.ac.cn*

Received February 26, 2012; accepted March 29, 2012; posted online April 24, 2013

A special-velocity-matched electro-optic (EO) phase modulator employing a microwave resonant design in lithium niobate is presented. Both the microwave property and phase-modulation performances of the 3.25-GHz modulator agree well with the numerical simulations. Using this modulator in a single-pass configuration with 1-kW microwave drive power, the spectral bandwidth of a 1 053-nm, 3-ns pulse-length laser is broadened to 0.13 nm. With a clear aperture of 5×5 (mm), the modulator is suited for two-dimensional smoothing by spectral dispersion in high power laser systems.

OCIS codes: 230.2090, 230.4110, 350.4010, 160.3730, 140.3580.
doi: 10.3788/COL201311.052301.

By high-frequency phase modulation, the bandwidth of single frequency laser is broadened for two major purposes in high power laser systems, such as SG-II, OMEGA, and NIF. Firstly, a 0.1-nm bandwidth is required to suppress the buildup of stimulated Brillouin scattering (SBS) in large aperture optics. Secondly, additional bandwidth of 0.3∼1 nm is required for the application of smoothing by spectral dispersion (SSD)[1]. These modulations could be generated by optical-waveguide phase modulators in master oscillators or bulk phase modulators in pre-amplifiers. Bulk phase modulator is a key component of two-dimensional (2D) SSD[2−4] by applying two separated stages of phase modulations and orthogonal dispersions to meet the beam smoothing requirements in direct drive inertial confinement fusion.

Bulk modulators for 2D SSD need to meet following requirements: 1) an appropriate clear aperture; 2) phase velocity match between the laser and the microwave; 3) a high microwave Q factor[5]. Currently, the clear aperture of the commercial bulk phase modulator[6] is about 1 mm, which is too small to meet the 2D SSD's requirement. Velocity-mismatch between microwave and laser limits the modulation efficiency. Two different modulator designs were proposed to resolve this problem. By using periodically-poled lithium tantalite, a quasi-velocity-matched phase modulator[7] was achieved. Such a phase modulator with a modulation index of 1.8 rad/kW at 9.4 GHz was used in three-dimensional SSD[8]. Meanwhile, higher Q factor and larger clear aperture were achieved by bulk modulators operating at TE_{10k} microwave resonant mode with velocity-matched design[9,11], where k is the longitudinal mode. A rigid-velocity-matched[12] phase modulator operating at 10.4 GHz was developed for 2D SSD in Omega.

In this letter, an efficient, special-velocity-matched microwave resonant phase modulator operating at TE_{101} resonant mode of 3.25 GHz is presented. The clear aperture is 5×5 (mm), which is the biggest reported aperture. In the modulator, microwave phase velocity is approximately 1.5 times of the laser velocity. Compared to a rigid-velocity-matched design, modulation efficiency of this special design is higher by about 12.8%.

When laser with a angular frequency of ω_0 is impressed by a sinusoidal phase modulation with a angular frequency of $\omega_{\rm m}$, the modulated laser electric field is given by[1]

$$E_{\rm opt}(t) = A{\rm e}^{{\rm i}(\omega_0 t+\delta\sin\omega_{\rm m}t)} = A\sum_{k=-\infty}^{+\infty} J_k(\delta){\rm e}^{{\rm i}(\omega_0+k\omega_{\rm m})t}, \qquad (1)$$

where $J_k(\delta)$ is Bessel function, k is any integer, and δ is modulation index. This expression implies that the laser temporal spectrum is broadened by sinusoidal phase modulation. The spectral bandwidth of phase-modulated laser is proportional to modulation index δ, approximately given by

$$\Delta f = \delta\omega_m/\pi. \qquad (2)$$

Due to the transverse electro-optic effect, a high frequency sinusoidal variation of the refractive index is obtained by coupling microwave signal into an EO crystal. When laser beam propagates along the y direction in Fig. 1(a), both the optic and microwave vectors are along the z axis, δ is given by

$$\delta = \beta L \times \left(\pi n_e^3 r_{33} E_m\right)/\lambda, \qquad (3)$$

Where L is the crystal length, $n_{\rm e}$ is the refractive index, r_{33} is the electro-optic coefficient, $E_{\rm m}$ is the electric field, λ is the laser wavelength in air and β is the velocity-mismatch reduction factor[13]. In the microwave resonant electro-optic phase modulator, standing microwaves are formed along the EO crystal, comprised of fields co-propagating and counter-propagating with the laser beam, and β is given by[13]

$$\beta = \left|\frac{\sin(u_+)}{u_+} + \frac{\sin(u_-)}{u_-}\right|, u_\pm = \frac{L\omega_{\rm m}}{2}\left(\frac{1}{\nu_{\rm opt}} \mp \frac{1}{\nu_{\rm rf}}\right), \qquad (4)$$

Table 1. Parameters of Lithium Niobate

EO Coefficient (pm/V)[14]	r_{33} =28.8–30.8
Refraction Index[14]	n_e =2.1561
Relative Dielectric Constant[15]	$\sqrt{\varepsilon_{11}}$ =6.64±0.06
	$\sqrt{\varepsilon_{33}}$ =5.11± 0.06
Loss Tangent[15]	0.004

where $\nu_{\rm opt}$, $\nu_{\rm rf}$ are the laser phase velocity and microwave phase velocity in the EO crystal along the propagation direction, respectively.

Lithium niobate ($LiNbO_3$) was chosen as the EO crystal, whose parameters are listed in Table 1. For a modulation frequency of 3.3 GHz, the relationship between effective crystal length (βL) and crystal length (L) under different velocity-matching conditions ($\nu_{\rm rf}/\nu_{\rm opt}$) is shown in Fig.2. Without velocity matching design (black light-solid curve), the maximum effective interaction length is limited to ~10 mm. Red heavy-solid curve is for a rigid-velocity-matched design, and there is a stage between L=10 and L=29 mm. In this area, if the microwave velocity is faster than laser velocity, effective crystal length is lengthened, for violet dash curve ($\nu_{\rm rf}/\nu_{\rm opt}$=1.3) and green dot curve ($\nu_{\rm rf}/\nu_{\rm opt}$=1.5). If the laser velocity is faster in this area, effective crystal length is shortened, for blue long-dash dot curve ($\nu_{\rm rf}/\nu_{\rm opt}$=0.7).

Schematic of a microwave resonant electro-optic bulk phase modulator is shown in Fig. 1 (a). Microwave is coupled into the EO crystal via a waveguide-coaxial adapter and a TE_{10}-mode waveguide. For EO crystal ($LiNbO_3$) has a much higher dielectric constant than air, cutoff frequency of the air-filled waveguide section is higher than the operating frequency. Thus, a microwave resonant cavity is formed at the EO crystal, working at a TE_{10k} mode. Compare to other bulk modulator designs, microwave resonant EO phase modulator has following advantages: 1) phase velocity matching between the laser and microwave is achieved by controlling the EO crystal dimension, modulator could operate at TE_{10k} resonant mode; 2) due to the high microwave Q factor, this modulator has much higher modulation efficiency.

The design of a microwave resonant EO phase modulator could be decomposed into the resonant cavity and the microwave coupling design[9]. Cavity design is achieved by setting the appropriate dimension of the crystal, shown in Figs. 1(b) and (c). Ignoring phase shifts associated with the reflections at the cutoff-waveguide, the length of the crystal is an integer multiple of half-wavelengths of the microwave. For a 3.3-GHz TE_{101} mode $LiNbO_3$ modulator with the velocity-matched design, crystal length is about 21 mm which is in the stage area shown in Fig. 2. In this area, microwave velocity could be faster than the laser. According to Fig. 2, $\nu_{\rm rf}/\nu_{\rm opt}$=1.3 is selected. The microwave phase velocity in the crystal is adjusted by setting the width of the crystal (w), given by[10]

$$\nu_{\rm rf} = \frac{c}{\sqrt{\varepsilon_{33}}\sqrt{1-(f_{\rm cutoff}/f_{\rm mod})^2}},$$
$$f_{\rm cutoff} = \frac{c}{2w\sqrt{\varepsilon_{33}}}, \qquad (5)$$

where $f_{\rm mod}$ is the operating frequency of the modulator, $f_{\rm cutoff}$ is the cutoff frequency of the crystal, and c is the light velocity in air. To match the laser velocity in the crystal, c/n_e, the crystal width is about 9.4 mm. To ensure the TE_{10} mode, the crystal height needs to meet the condition of $c/2h\sqrt{\varepsilon_{33}} < 3.3$ GHz. Considering the clear aperture requirement of SSD, h is set 5 mm. Except for the two clear aperture, all the other four sides of the crystal are gold coated. The transverse section of the cutoff waveguide is a bit larger than the $LiNbO_3$ crystal.

In Fig. 1 (a), the input waveguide consisted of a waveguide coaxial adapter, an E-plane tapered waveguide and an E-plane waveguide bend. By the tapered waveguide, the height of the waveguide is shortened from the standard 34 to 10 mm. An isotropic numerical simulation is performed by using electromagnetic

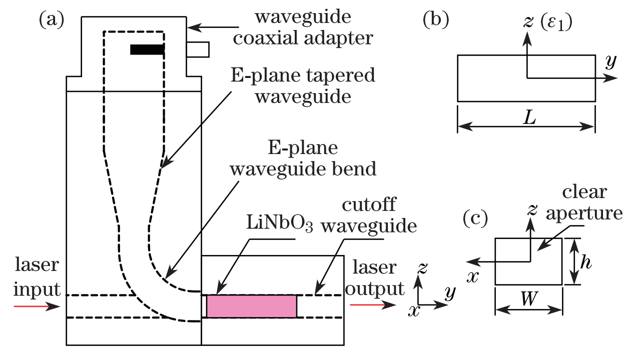

Fig. 1. Schematic of a microwave resonant electro-optic bulk phase modulator.

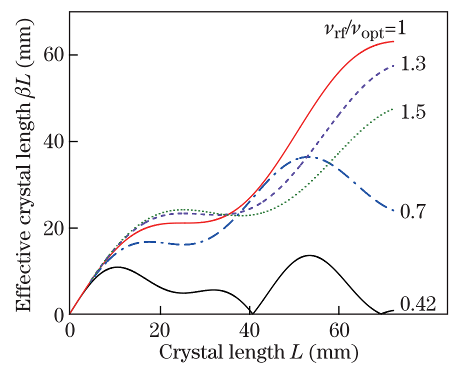

Fig. 2. Relationship between effective crystal length and original crystal length for different velocity-matching conditions.

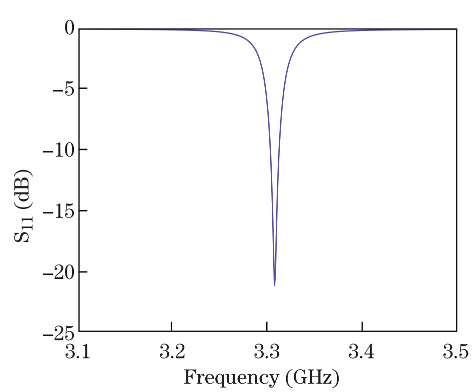

Fig. 3. Simulated microwave reflectivity versus frequency.

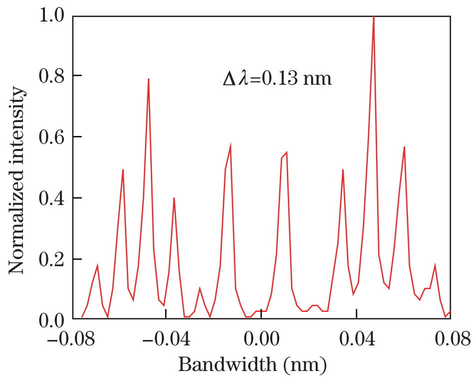

Fig. 4. Spectra measured by a single-pass phase-modulation using FP etalon.

simulation software. To increase the coupling efficiency, the crystal is extended into the input waveguide for 2 mm. According to the simulation result, TE_{101} resonant frequency of 3.32 GHz is achieved when the crystal length is 18 mm with a Q factor of 114.5. The simulated microwave reflectivity versus frequency bandwidth from 3.1 to 3.5 GHz is plotted in Fig. 3. The results indicate that the modulator has a high microwave coupling efficiency at the TE_{101}.

The microwave properties of the modulator were measured by a microwave vector network analyzer. TE_{101} mode of 3.25 GHz and corresponding $S_{11}$of −18 dB was achieved for an extending distance of ∼1.8 mm with a Q factor of 118. The resonant frequency of 3.25 GHz is lower than simulated results by 2.1%, and the measured Q factor is higher than simulated results by 3%. Compare to the design of 3.3 GHz, the actual phase velocity of the microwave is higher than the design value from Eq. (5) by 16.7%. Thus, the real velocity-matching condition is $\nu_{\rm rf}/\nu_{\rm opt}$=1.5, whose effective length was predicted by green dot curve in Fig. 2 with a β of 1.32. The cause of the inconsistent between the tested frequency and simulated value are as follows: First, the actual dielectric constant of the $LiNbO_3$could differ from the simulations. Second, to integrate the $LiNbO_3$, the actual cutoff waveguide is a bit larger than the simulations.

A Fabry-Perot (FP) etalon with a free spectral range (FSR) of 60 GHz at 1 053 nm was used to measure the phase-modulation performance. Using the modulator in a single-pass modulation configuration with 1-kW microwave drive power, the spectral bandwidth of a 1 053-nm, 3-ns pulse-length laser is broadened to 0.13 nm, as shown in Fig. 4. The respective modulation index δ is 5.4. While, the modulation index could be predicted by[10]

$$\delta_{\rm mod} = \frac{\pi n_{\rm e}^3 r_{33} N\beta L}{\lambda_{\rm opt}}\sqrt{\frac{2Q_0 P_{\rm in}}{\varepsilon_{33}\omega_m w h L}}, \qquad (6)$$

where Q_0 is the Q factor, $P_{\rm in}$ is the microwave power, and N is the number of pass. The predicted modulation index is 5.15, which agrees well with the measurement. Compared to a rigid-velocity-matched design with a β of 1.17 in Fig.2, modulation efficiency of this optimized-velocity-matching design is higher by 12.8%. Because $\delta_{\rm mod} \propto \sqrt{P_{\rm in}}$, to get the same modulation index, the required microwave power could decrease by 21.5%.

In conclusion, an efficient, special-velocity-matched microwave resonant bulk phase modulator operated at TE_{101} resonant mode of 3.25 GHz is successfully developed. Both the microwave properties and phase-modulation performances agree well with the numerical prediction. By the optimized velocity-matching design, a velocity-mismatch reduction factor β of 1.32 is expected, which is higher than a rigid-velocity-matched design by 12.8%. Using this modulator in a single-pass configuration with 1-kW microwave drive power, the spectral bandwidth of a 1 053-nm, 3-ns pulse-length laser is broadened to 0.13 nm. With a clear aperture of 5×5 (mm), the modulator is suited for 2D SSD in high power laser systems.

References

1. S. Skupsky, R. W. Short, T. Kessler, R. S. Craxton, S. Letzring, and J. M. Soures, J. Appl. Phys. **66,** 3456 (1989).
2. S. Skupsky and R. S. Craxton, Phys. Plasmas **6,** 2157 (1999).
3. S. P. Regan, J. A. Marozas, J. H. Kelly, T. R. Boehly, W. R. Donaldson, P. A. Jaanimagi, R. L. Keck, T. J. Kessler, D. D. Meyerhofer, W. Seka, S. Skupsky, and V. A. Smalyuk, J. Opt. Soc. Am. B **17,** 1483 (2000).
4. S. P. Regan, J. A. Marozas, R. S. Craxton, J. H. Kelly, W. R. Donaldson, P. A. Jaanimagi, D. J. Perkins, R. L. Keck, T. J. Kessler, D. D. Meyerhofer, T. C. Sangster, W. Seka, V. A. Smalyuk, S. Skupsky, and J. D. Zuegel, J. Opt. Soc. Am. B **22,** 998 (2005).
5. D. Kajfez, *Q Factor* (Vector Fields, Oxford, MS, 1994).
6. A. A. Godil, U.S. Patent 5, 414, 552 (1995).
7. F. Z. Guo, C. T. Yu, L. Chen, T. Kobayashi, and Y. Chen, IEEE J. Quantum Electron. **33,** 879 (1997).
8. G. Miyaji, N. Miyanaga, S. Urushihara, K. Suzuki, S. Matsuoka, M. Nakatsuka, A. Morimoto, and T. Kobayashi, Opt. Lett. **27,** 725 (2002).
9. E. Bonek, M. Knecht, G. Magerl, K. Preis, and K. R. Richter, Arch. Elektr. Uebertrag. **32,** 209 (1978).
10. T. F. Gallagher, N. H. Tran, and J. P. Watjen, Appl. Opt. **25,** 510 (1986).
11. N. H. Tran, T. F. Gallagher, J. P. Watjen, G. R. Janik, and C. B.Carlisle, Appl. Opt. **24,** 4282 (1985).
12. J. D. Zuegel and D.W. Jacobs-Perkins, Appl. Opt. **43,** 1946 (2004).
13. I. P. Kaminow and J. Liu, Proc. IEEE **51,** 132 (1963).
14. R. S. Weis and T. K. Gaylord, Appl. Phys. A **37,** 191 (1985).
15. W. M. Robertson, G. Arjavalingam, and G. V. Kopcsay, Electron. Lett. **27,** 175 (1991).